Research Article | **Open Access**

Nano Size Related Piezoelectric Efficiency in a Large ZnO Thin Film, Potential for Self-Powered Medical Device Application

YuTong Li, Zhiqang Gao, Wei Wei Qin, Qiu Jun Wen, Ma Xian Jun, Wei Du, Xiaoqiang Chen, Hu Xue Feng* and Wei Zhang*

State Key Laboratory of Material-oriented Chemical Engineering and School of Chemical Engineering, Nanjing Tech University, PR China

Abstract

Large-area piezoelectric ZnO films with different gran size has been synthesized by sol-gel technique using different annealing temperatures from 550 to 700°C. The piezoelectric efficiency (PE) of those deposited films is characterized by Piezoelectric Force Microscopy (PFM). All synthesized films exhibit a crystal structure. The width of the rock curve of [0002] characterized by x-ray diffraction decreases with the annealing temperature, suggesting a better c-axis orientated ZnO film formed at higher annealing temperature. The grain size of the grown films are found to continuously increase from 20 to 60 nm when the annealing temperatures increase from 550 to 700°C. The piezoelectric efficiency (PE, d_{33}) of the films exhibit strong grain size dependence, i.e., the PE initially increase with the annealing temperature and then decreasing with a further annealing temperature increased. The maximum PE value appears in the film annealed at 650°C. The peculiar piezoelectric properties (d_{33}) can be explained by the competing between the crystalline, which favors a larger d_{33} due to the enhanced dipole polarization, and the grain size, which results in a piezoforce release at large grain size due to domain wall size and motion.

Keywords: Grain Size; Sol-gel; Nanogenerator; ZnO thin film; Piezoelectric efficiency; Biosensor

Introduction

In vivo sensors have a wide application for real-time biomedical monitoring [1]. Single-use or non-rechargeable batteries to support implanted device limits the application of those promising implanted sensors, because of requiring to be surgically replaced at the end. The human body, in fact, is a natural power source, owning potential energy such as chemical energy (glucose), hydraulic energy (body fluid and blood flow), and blood vessel contraction). The challenges remaining are how to efficiently convert them into electrical energy [2]. The nanogenerator based on ZnO nanowire has demonstrated to enable the collection of the energy from the environmental mechanical energy and to drive electrical device in the microwatt power range [3-6]. The fundamental mechanism of a nanogenerator (NG) is related to a piezoelectric potential generated in nano wire (NW) under an external force, and a current flows on a loading resistor [7,8]. Although such prototyping work has demonstrated the basic principle of the nanogenerator, the performance must drastically improve to make nanogenerators for practical applications. NG process must be low cost and easy for mass production. Thus, it is necessary to develop strategies towards achieving cost-effective NG in order to consistently scavenge the mechanical energy from the environmental sources.

Piezoelectric thin film power generator has emerged as a promising candidate for vibrating energy collector [9-12]. Recently, high power output from lead zirconate titanate (PZT) piezoelectric thin films onto flexible substrates has suggested a direct application of piezoelectric films as piezoelectric generators without the requirement of NW fabrication [6]. In comparison with NW-type nanogenerators, thin film nanogenerators possess numerous advantages, simple and mature process, well-controlled film properties, and, more important, compatibility with current semiconductor IC technology for mass production [13-15].

A number of techniques, chemical vapor deposition [16], spray-pyrolysis [17], molecular beam epitaxy [18], vacuum arc deposition [19], magnetron sputtering [20-22] and pulsed laser deposition (PLD) [23], have been involved in the growth of ZnO thin films. Sol-gel method has emerged as an important growth technique because it enables the

surface modification of zinc oxide with selected organic compounds. It can offer simplicity and low cost mild conditions of synthesis required by large-scale nanogenerator application [23]. In this paper, we prepare ZnO film on Si substrate by Sol-gel technique. Different film structure and grain sizes of ZnO thin films were generated by post-annealing at different temperatures from 550 to 700°C. Structurally, emphasis is placed on XRD characterization of the films. The grain size of the films was characterized using Atomic Force Microcopy (AFM) and Scanning Electron Microscopy (SEM). The local piezoelectric properties of these films are obtained using PFM. The observed relationship between the piezoelectric (PE) property and the film structure is theoretically explained.

Materials and Methods

To performance PFM characterization, Pt bottom electrodes with 5 nm in thickness were prepared on 6-inches Si (100) substrates using vacuum thermal evaporation. The 0.35M ZnO precursor solution was gained by dissolving high-purity zinc acetate dehydrate (Zn (CH_3COO)_2·2H_2O, 99.0%) in 2-methoxyethanol (C_3H_8O_2, 99.0%). When the solution stirred at 60°C for 2h, the monoethanolamine (MEA, C_2H_7NO, 99.0-100.3%) was slowly added into the solution as a stabilizer which makes the solution clear. The molar of ratio MEA to zinc acetate

*Corresponding authors: Wei Zhang, State of Key Laboratory of Materialsoriented Chemical Engineering and School of Chemical Engineering, Nanjing Tech University, Nanjing, Jiangsu, 210009, PR China, Tel: 86 25-83587060; E-mail: zhangw@njtech.edu.cn

Xuefeng Hu, State of Key Laboratory of Materials-oriented Chemical Engineering and School of Chemical Engineering, Nanjing Tech University, Nanjing, Jiangsu, 210009, PR. China, E-mail: xuefeng.hu@njtech.edu.cn

was kept at 1.0. The solution is then aged for more than 24h at room temperature before it is used. For ZnO film growth, the Pt/Si substrates are in-turn cleaned in an ultrasonic bath with acetone, ethanol, and distilled water. Then, Pt/Si substrates were dried in nitrogen and ready for coating. The precursor solution is spin-coated on the Pd/Si (100) substrates at 3000 rpm for 30s. After each coating, the as-coated film is preheated from room temperature to 350°C for 10 minutes. The spin-coating and preheating process was repeated six times to make a dense film with a 70 nm in thickness. Finally, the films are annealed at 550°C, 600°C, 650°C and 700°C in air for 1hour in a quartz-tube furnace.

The structure of the deposited film is determined using XRD analyses with a Philips PW3710 system (Cu-Kα radiation, λ=0.15406 nm). AFM (Oxford A350) is using to characterize the morphology of the films. The grain size of the films is characterized using XRD and Scanning Electron Microscopy (Hitachi 7800, 20 keV). PFM (Oxford A350) is a similar to typical contact mode imaging tool, except an AC voltage is applied to the surface of a piezoelectric sample through the tip of a conductive AFM cantilever. When a voltage is applied, the piezoelectric thin film undergoes a change in shape, leading to a change in tip-to-surface height. This height change can be tracked and measured with a piece of equipment called a lock-in amplifier, which tracks the contact resonance frequency of the tip-to-surface contact.

Results

Figure 1 shows a XRD pattern for the film annealing at various temperatures and the details are summarized in Table 1. The XRD spectra of all four samples exhibit a strong (002) peak, which indicates that they have a preferential growth orientation along the c-axis perpendicular to the substrate surface. As the annealing temperature is increased, the relative intensity of the (002) diffraction peak increases rapidly and its full width at half maximum (FWHM) decreases gradually. Regarding the ZnO film grown at 700°C, the intensity of the (002) diffraction peak is maximum and its full width at half maximum (FWHM) is found to be 0.26°C. These results indicate that the crystallinity of the ZnO thin films is enhanced as the annealing temperature is increased. Using the Scherrer formula, $D_{XRD}=0.94\lambda/(\beta\cos\theta_\beta)$ (where λ, θ_β, and β are the x-ray wavelength, the Bragg diffraction angle, and the line width at half maximum of the diffraction peak, respectively), the mean crystallite sizes (D_{XRD}), as presented in the Table 1, are calculated to be 27.0, 28.7, 30.9 and 34.7 nm for the films annealed at 550, 600. 650, 700°C, respectively.

Figure 1: XRD diffraction patterns of the ZnO films prepared by Sol-gel on Si (100) substrates and annealed in the temperature range from 550°C to 700°C.
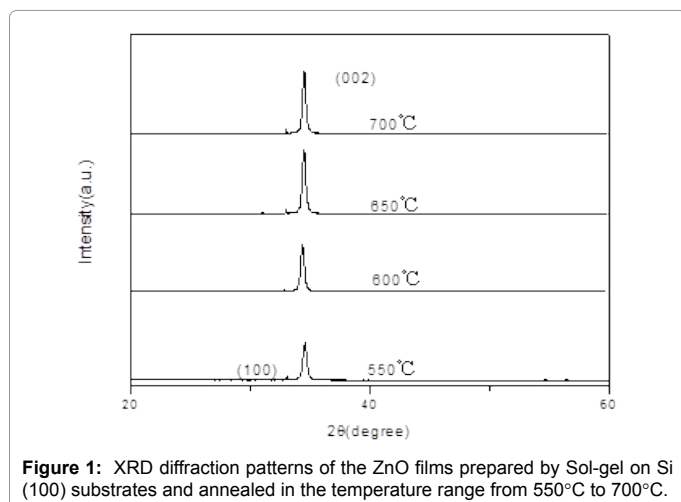
Substrate	Annealing temperature (°C)	2θ (deg)	FWHM (deg)	Grain size (nm)
Si(100)	550	34.560	0.324	27.0
	600	34.600	0.307	28.7
	650	34.600	0.287	30.9
	700	34.599	0.260	34.7

Table 1: Data summary of the peak position, full width at half maximum (FWHM) and calculated grain size at various annealing temperatures.

Figure 2: Cross-sectional dark-field TEM images and electron diffraction pattern (inset) of the ZnO film annealing at 650°C.

Figure 3: SEM images of the ZnO thin films annealed at (a) 550°C; (b) 600°C; (c)650°C; and (d) 700°C.
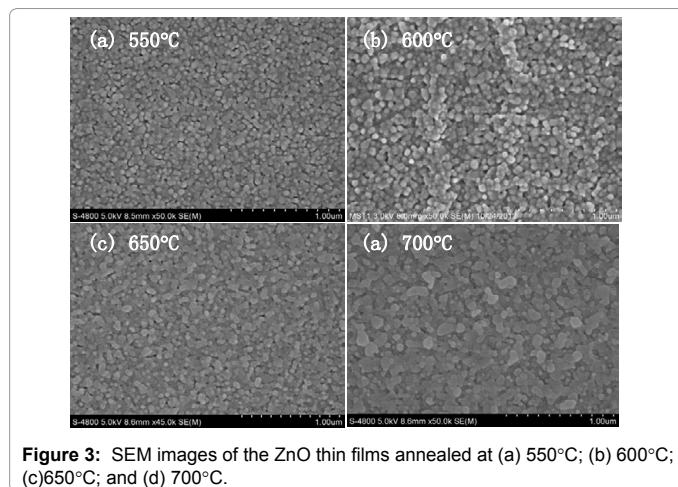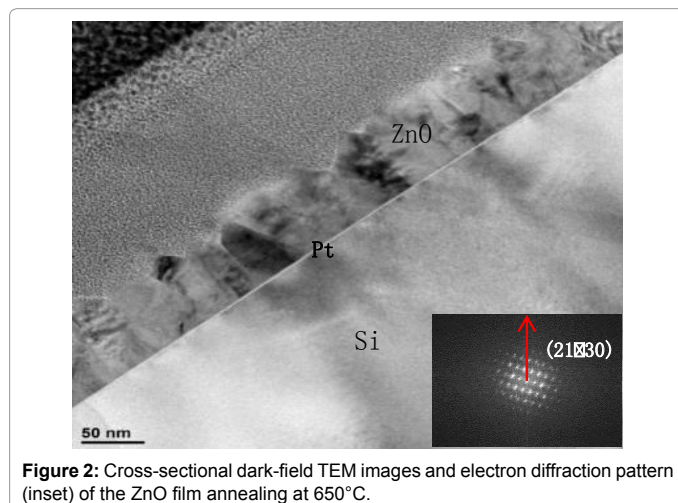
Figure 2 shows a typical cross-sectional dark-field TEM micrographs of a ZnO film on a Si substrate annealed at 650°C. The thickness of the film obtained from the TEM image is approximately 70 nm. Columnar growth can be clearly observed for the film deposited on the Si substrate. The shape of the grains in the upper region of the structure is convex, because the upper region is more stable and closer to equilibrium morphology due to atomic mobility and stress relaxation, in compared to the lower region [24]. The inset of Figure 2 shows the selected area electron diffraction data obtained with the electron beam parallel to the [21 30] zone axis of ZnO. The indexed diffraction pattern confirms the hexagonal structure of the ZnO thin film.

The average grain size at film surface with a data more accuracy of ±4 nm is also characterized by SEM. Figure 3 shows that the grain size of the film increases with the annealing temperature. A comparison of Figures 4a and 4d clearly indicates that the larger grains have sharper interfaces, while the smaller grains are separated by distinct inter-
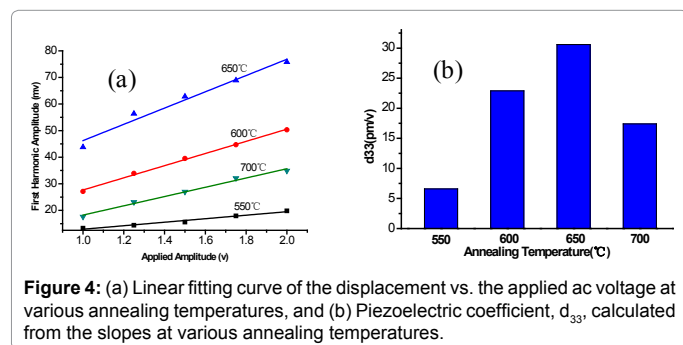
Figure 4: (a) Linear fitting curve of the displacement vs. the applied ac voltage at various annealing temperatures, and (b) Piezoelectric coefficient, d_{33}, calculated from the slopes at various annealing temperatures.

granular regions, in particular for the samples with smaller average grain sizes. Because these images show only grains with a particular crystallographic orientation, so individual grains can be identified. The grain size characterized by SEM is typically in close agreement with the calculated values of d_{XRD} in grain size trend. We can identify a couple of grains in which the crystalline order persists for ~ 8-9 nm. The width of the inter-granular region is ~ 5 nm in this film. This type of grain boundary is structurally similar to that recently observed in ZnO films [25].

The Piezoelectric Effect (PE) of thin ZnO films is characterized by PFM for standard piezoelectric phenomena [26]. In all the piezoelectric measurements, the interaction between the tip and electric field was ignored [27]. The displacement as a function of applied voltage for the films is shown in Figure 4a. The amount of the displacement under an AC voltage, which does not follow the trend of grain size and c-axis orientation, initially increases with grain size and then decreases when the annealing temperature is further increased. The maximum displacement point appears for the film annealed at 650°C. The piezoelectric coefficient d_{33}, as showed in Figure 4b, can be determined from the slope of the resulting plot of the amplitude of displacement *vs.* that of applied voltage, which represents peak-to-peak values of both the displacement and the applied voltage. To reference the piezoelectric response to the piezoelectric material, the PE response on a bare single crystalline Si (100) substrate is also calculated. The piezoelectric constant d_{33} is approximately 0.26 pm/V for the bare Si substrate, which is at a similar level (<0.5 pm/V) as the value in the reference literature [28,29]. As a result, the impact of initial substrate roughness on the PE result can be ignored. The piezoelectric constant for the ZnO thin film initially increases from 6.5 pm/V to 32.5 pm/V when the annealing temperature increases from 550 to 650°C. The piezoelectric constant then decreases to 17 pm/V when the annealing temperature further increases to 700°C. A maximum PE value of 32.5 pm/V appears for the film annealed at 650°C.

The peculiar behavior of the PE constant at different grain sizes may be primarily attributed to competing effects between the grain size and the c-axis orientation of the ZnO films. ZnO's wurtzite structure has a hexagonal unit cell of space group *C6mc* and lattice parameters $a = 0.3296$ and $c = 0.52065$ nm. The oxygen anions and Zn cations form a tetrahedral unit. The entire structure lacks central symmetry. The structure of ZnO can be simply described as a number of alternating planes composed of tetrahedrally coordinated O^{2-} and Zn^{2+} ions stacked alternatively along the c-axis. Although the entire unit cell of ZnO is neutral, the distribution of the cations and anions could adopt a specific configuration determined by crystallography such that some surfaces can be terminated entirely with cations or anions, resulting in positively or negatively charged surfaces or polar surfaces. The most common polar surface is the basal plane. The oppositely charged ions produce positively charged Zn- (0001) and negatively charged O-(0002) polar

surfaces, resulting in a normal dipole moment and spontaneous polarization along the c-axis as well as a divergence in the surface energy[30-32]. More c-axis oriented film growth at a high annealing temperature diminishes the d spacing along the c-axis and enhances ZnO polarity, leading to a high PE constant.

Grain size is an important factor in affecting on the piezoelectric properties [33-36]. Obviously, the film stress plays a role in piezoelectric property, but cannot explain the dependence of d_{33} on the grain size observed in our experiment because of the maximum d_{33} appearing in the ZnO film annealed at 650°C. The reduction of the ratio c/a with the reduction of the grain size cannot also explain the strong grain-size dependence of d_{33} because it is related directly to the decrease of spontaneous polarization. Accordingly, an intrinsic mechanism related to ion shift, which preserve the piezoelectric crystal structure, used to explain for the observed behavior is not likely. In contrast, the coupling between the grains and the motion of the domain walls are considered to very likely provide a dominating contribution to the observed behavior. At a case of small grain, the direction of spontaneous polarization is aligned opposing among neighbor grain, which is caused by strong coupling due to narrow grain boundary. Therefore the collective piezoelectric response is small, because the spontaneous polarization is cancelled each other. When the grain grow, the coupling interaction among grains is weakened, but external force can be released at wide grain boundary, leading a decrease in piezoelectric response. Therefore an optimum grain size can result in a maximum PE. Some similar studies are previously carried out [37-40]. The domain wall density has been considered as the origin of the strong dielectric grain-size dependence of ε' observed in unpoled ferroelectric $BaTiO_3$ ceramics [37] and of the large enhancement in d_{33} observed in poled fine-grained $BaTiO_3$ ceramics [38-40]. In addition, the area dimension of the 90°-domain wall should also be an important factor that greatly influences d_{33} [41-43]. This behavior is well-consistent with the PE value of the ZnO films observed at different grain sizes exhibit size-dependent PE behavior and d_{33} values [44].

Conclusion

In this paper, high-quality ZnO thin films with preferred c-axis orientation are prepared on single-crystal Si (100) via sol-gel growth method and then annealed in the temperature range of 550 to 700°C. XRD, SEM and PFM are utilized for the characterization of structural and piezoelectric properties. While all films annealed in the temperature range of 550 to 700°C exhibit c-axis orientation, the films with higher annealing temperatures are grown with larger grain sizes simultaneously. The piezoelectric efficiency of the films initially increases with the grain size and then decreases with further increase in grain size. The peculiar piezoelectric properties (d_{33}) can be explained by the competition between c-axis orientation, which favors a larger d_{33} due to enhanced static asymmetry, and grain size, which is likely related to motion of domain wall. ZnO films with high PE values are potential candidates for building nanogenerator for energy harvesting applications.

References

1. Majerus SJA, Garverick SL, Suster MA, Fletter PC, Damaser MS (2012) Wireless, ultra-low-power implantable sensor for chronic bladder pressure monitoring. J. Emerg. Technol. Comput. Syst 8: 1-13.

2. Rapoport BI, Kedzierski JT, Sarpeshkar R (2012) A glucose fuel cell for implantable brain-machine interfaces. PLoS One 7.

3. ZL Wang, Nanotoday (2011) Nanogenerators for Self-powered Devices and Systems (1stedn) Georgia Institute of Technology.

4. Yu Y, Zhao P, Jiang ZL, Wang (2013) A nanogenerator as a self-powered sensor for measuring the vibration spectrum of a drum membrane. Nanotechnology, 24: 055501.

5. Wang ZL, Song JH (2006) Piezoelectric Nanogenerators Based on Zinc Oxide Nanowire Arrays. Science 312: 242-246.

6. Wu WZ, Wei YG, Wang ZL (2010) "Strain-gated piezotronic logic nanodevices" Adv. Mater 22: 4711-4715.

7. Xu S, Qin Y, Xu C, Wei Y, Yang R, et al. (2010) Self-powered nanowire devices. Nature Nanotechnology 5: 366-373.

8. Du CL, Gu ZB, You YM, Kasim J, Yu T, et al. (2008) Resonant Raman spectroscopy of (Mn,Co)-codoped ZnO films. Journal of Applied Physics 103: 023521.

9. Lee S, Hong J, Xu C, Lee M, Kim D, et al. (2012) "Toward robust nanogenerator using aluminum substrate." Advanced Materials 24: 4398-4402.

10. Hu Y, Zhang Y, Xu C, Lin L, Snyder RL, et al. (2011) Self-powered system with wireless data transmission. Nano Lett 11: 2572-2577.

11. Gardeniers JGE, Rittersma ZM, Burger GJ (1998) Preferred orientation and piezoelectricity in sputtered ZnO films. J Appl Phys 83: 7844.

12. Kamohara T, Akiyama M, Ueno N, Sakam-oto M, Kano K, et al. (2006) Influence of sputtering pressure on polarity distribution of aluminum nitride thin films. Appl Phys Lett 89: 243507.

13. Kamohara T, Akiyama M, Kuwano N (2008) Influence of polar distribution on piezoelectric response of aluminum nitride thin films. Appl Phys Lett 92: 093506.

14. Chang CE, Tran VH, Wang JB, Fuh YK, Lin LW (2010) Direct-Write Piezoelectric Polymeric Nanogenerator with High Energy Conversion Efficiency. Nano Lett 10: 726.

15. Cha S, Kim SM, Kim H, Ku J, Sohn JI, et al. (2011) Porous PVDF as effective sonic wave driven nanogenerators. Nano Lett 11: 5142-5147.

16. Cho SH (2009) Effects of Growth Temperature on the Properties of ZnO Thin Films Grown by Radio-frequency Magnetron Sputtering. Trans Electr Electron Mater 10: 185-188.

17. Alam MJ, Cameron DC (2001) Preparation and properties of transparent conductive aluminum-doped zinc oxide thin films by sol–gel process. J Vac Sci Technol A 19: 1642.

18. Fiddes AJC, Durose K, Brinkman AW, Woods J, Coates PD, et al. (1996) Preparation of ZnO films by spray pyrolysis. J Cryst Growth 159: 210-213.

19. Ohgaki T, Ohashi N, Kakemoto H, Wada S, Adachi Y, et al. (2003) Growth condition dependence of morphology and electric properties of ZnO films on sapphire substrates prepared by molecular beam epitaxy. J Appl Phys 93: 1961-1965.

20. Ryu YR, Zhu S, Budai JD, Chandrasekhar HR, Miceli PF, et al. (2000) Optical and structural properties of ZnO films deposited on GaAs by pulsedlaser deposition. J Appl Phys 88: 201-204.

21. Minami T, Ida S, Miyata T (2002) High rate deposition of transparent conducting oxide thin films by vacuum arc plasma evaporation. Thin Solid Film 416: 92-96.

22. Kim KH, Park KC, Ma DY (1997) Structural, electrical and optical properties of aluminum doped zinc oxide films prepared by radio frequency magnetron sputtering. J Appl Phys 81: 7764-7772.

23. Willmott PR, Huber JR (2000) Pulsed laser vaporization and deposition. Reviews of Modern Physics 72: 315.

24. Shin JW, Lee JY, Kim TW, No YS, Cho WJ, et al. (2006) Growth mechanisms of thin-film columnar structures in zinc oxide on p-type silicon substrates. J Appl Phys 88: 091911.

25. Wang XB, Song C, Li DM, Geng KW, Zeng F, et al. (2006) The influence of different doping elements on microstructure, piezoelectric coefficient and resistivity of sputtered ZnO film. Appl Surf Sci 253: 1639-1643.

26. Li CP, Yang BH (2011) Local Piezoelectricity and Polarity Distribution of Preferred c-Axis-Oriented ZnO Film Investigated by Piezoresponse Force Microscopy. Journal of electronic materials 40: 253-258.

27. Bonnell A, Kalinin SV, Kholkin AL, Gruverman A (2009) Piezoresponse Force Microscopy: A Window into Electromechanical Behavior at the Nanoscale 9: 648-657.

28. Wang XB, Song C, Li DM, Geng KW, Zeng F, et al. (2006) The influence of different doping elements on microstructure, piezoelectric coefficient and resistivity of sputtered ZnO film. Appl Surf Sci 253: 1639-1643.

29. Christman JA, Woolcott RR, Kingon AI, Nemanich RJ (1998) Piezoelectric measurements with atomic force microscopy. Appl Phys Lett 73: 3851.

30. Dulub O, Diebold U, Kresse G (2003) Novel Stabilization Mechanism on Polar Surfaces: ZnO(0001)-Zn. Phys Rev Letts 90: 016102.

31. Wander A, Schedin F, Steadman P, Norris A, McGrath R, et al. (2001) Stability of Polar Oxide Surfaces. Phys Rev Letts 86: 3811.

32. Staemmler V, Fink K, Meyer B, Marx D, Kunat M, et al. (2003) Stabilization of polar ZnO-surfaces: Validating microscopic models by using CO as a probe molecule. Phys Rev Letts 90: 106102.

33. Bose S, Banerjee R, Genc A, Raychaudhuri P, Fraser HL, et al. (2006) Size induced metal insulator transition in nanostructured Niobium thin films: Intragranular and intergranular contributions. J Phys: Condens Matter 18: 4553-4566.

34. Zheng P, Zhang JL, Tan YQ, Wang CL (2012) Grain-size effects on dielectric and piezoelectric properties of poled BaTiO3 ceramics. Acta Mater 60: 5022-5030.

35. Zhang QM, Wang H, Kim N, Cross LE (1994) Direct evaluation of domain-wall and intrinsic contributions to the dielectric and piezoelectric response and their temperature dependence on lead zirconate-titanate ceramics. J Appl Phys 75: 454-459.

36. Demartin M, Damjanovic D (1996) Dependence of the direct piezoelectric effect in coarse and fine grain barium titanate ceramics on dynamic and static pressure. Appl Phys Lett 68: 3046-3048.

37. Hoshina T, Kigoshi Y, Hatta S, Teranishi T, Takeda H, et al. (2010) Size Effect and Domain-Wall Contribution of Barium Titanate Ceramics. Ferroelectrics 402: 29-36.

38. Takahashi H, Numamoto Y, Tani J, Matsuta K, Qiu J, et al. (2006) Lead-Free Barium Titanate Ceramics with Large Piezoelectric Constant Fabricated by Microwave Sintering. Jpn J Appl Phys 45: 30-32.

39. Karaki T, Yan K, Adachi M (2007) Lead-Free Piezoelectric Ceramics with Large Dielectric and Piezoelectric Constants Manufactured from BaTiO3 Nano-Powder. Jpn J Appl Phys 46: 7035-7038.

40. Zheng P, Zhang JL, Shao SF, Tan YQ, Wang CL (2009) Piezoelectric properties and stabilities of CuO-modified Ba(Ti,Zr)O3 ceramics. Appl Phys Lett 94: 032902.

41. Shao SF, Zhang JL, Zhang Z, Zheng P, Zhao ML, et al. (2008) High Piezoelectric Properties and Domain Configuration in BaTiO3 Ceramics Obtained Through the Solid-State Reaction Route. J Physics D: Appl Phys 41: 125408.

42. Randall CA, Kim N, Kucera JP, Cao WW, Shrout TR (1998) Intrinsic and Extrinsic Size Effects in Fine-Grained Morphotropic-Phase-Boundary Lead Zirconate Titanate Ceramics. J Am Ceram Soc 81: 677-688.

43. Damjanovic D (2005) Contributions to the piezoelectric effect in ferroelectric single crystals and ceramics. J Am Ceram Soc 88: 2663-2676.

44. Ma N, Zhang BP, Yang WG, Guo D (2012) Phase structure and nano-domain in high performance of BaTiO3 piezoelectric ceramics. J Eur Ceram Soc 32: 1059-1066.